J Korean Soc Appl Biol Chem (2013) 56, 11–20
DOI 10.1007/s13765-012-2177-3

ORIGINAL ARTICLE

Optimization of Process Variables for the Synthesis of Silver Nanoparticles by *Pycnoporus sanguineus* using Statistical Experimental Design

Yen San Chan · Mashitah Mat Don

Received: 13 August 2012 / Accepted: 14 December 2012 / Published Online: 28 February 2013

Abstract Sequential optimization strategy based on statistical experimental design and one-factor-at-a-time (OFAT) method were employed to optimize the process parameters for the enhancement of silver nanoparticles (AgNPs) production through biological synthesis using *Pycnoporus sanguineus*. Based on the OFAT method, three significant components influencing the size of AgNPs produced were identified as $AgNO_3$ concentration, incubation temperature, and agitation speed. The optimum values of these process parameter for the synthesis of AgNPs were determined using response surface methodology (RSM) based on Box-Behnken design. The validity of the model developed was verified, and the statistical analysis showed that the optimum operating conditions were 0.001 M of $AgNO_3$, 38°C, and 200 rpm with the smallest AgNPs produced at 14.86 nm. The disc diffusion method also suggested that AgNPs produced using optimum conditions have higher antimicrobial activity compared to the un-optimized AgNPs. The present study developed a robust operating condition for the production of AgNPs by *P. sanguineus*, which was 8.6-fold smaller than that obtained from un-optimized conditions.

Keywords Box-Behnken · optimization · *Pycnoporus sanguineus* · silver nanoparticles (AgNPs)

Introduction

Although silver nanoparticles (AgNPs) have been commercially produced using chemical synthesis such as chemical reduction (Khanna et al., 2005), photoreduction (Jia et al., 2006), micro-emulsion (Rao and Geckeler, 2011), γ-radiation (Long et al., 2007), electrochemistry (Yu et al., 2010), and supercritical liquid (Chang et al., 2003), arrays of physical, chemical, and biological methods have been studied for nanoparticle synthesis. AgNPs prepared by physical and chemical approaches have shown superior properties; however, most of these methods relied heavily on the use of organic solvent and toxic-reducing agents such as *N,N*-dimethylformamide, hydration hydrazine, and sodium borohydride. The use of these toxic chemicals are subject of paramount concern (Vigneshwaran et al., 2006). Therefore, developing an environmentally benign process for the synthesis of AgNPs deserves merit. Microbial synthesis seems to be a promising alternative as it is regarded as an eco-friendly and sustainable approach in synthesizing AgNPs.

Various species of microorganisms have been utilized in synthesizing AgNPs either intracellularly (Meyer et al., 2010; Greulich et al., 2011) or extracellularly (Ahmad et al., 2003b; Bhainsa and D'Souza, 2006b; Kalishwaralal et al., 2008; Balaji et al., 2009). Interactions between microbes and metals have been exploited in microbial detoxification. It is understood that microbial resistance to most toxic heavy metals are due to chemical detoxification by membrane proteins that function either as ATPase, chemiosmotic cation, or proton anti-transporters (Beveridge et al., 1996; Bruins et al., 2000). In fact, synthesis of AgNPs can be conducted by biomineralization, biosorption, complexation or precipitation (Klaus-Joerger et al., 2001). Previous works reported that bacteria strains such as *Klebsiella pneumonia* (Mokhtari et al., 2009), *Bacillus licheniformis* (Kalimuthu et al., 2008), *Bacillus subtilis* (Kannan et al., 2011), *Escherichia coli* (Gurunathan et al., 2009) are capable of synthesizing AgNPs. Recently, fungi, which were more advantageous compared to other microorganisms have been explored for AgNPs synthesis. Among them, *Fusarium oxyporum* (Ahmad et al., 2003a), *Aspergillus niger* (Gade et al., 2008), and *Aspergillus fumigatus* (Bhainsa and D'Souza, 2006a) were the most studied strains due

C. Yen San · M.D. Mashitah (✉)
School of Chemical Engineering, Universiti Sains Malaysia Engineering Campus, 14300 Nibong Tebal, Seberang Perai Selatan, Penang, Malaysia
E-mail: chmashitah@eng.usm.my

to their extracellular secretion in nature. Fungal mycelial has the ability to withstand high flow pressure and agitation, resulting in easier handling of fungi cultivation in a large scale bioreactor. Rajesh Kumar et al. (2012) also reported that fungi strains produce nanoparticles extracellularly due to their enormous secretary components that is crucial in the reduction process. The reductive proteins were secreted extracellularly during the synthesis of AgNPs; hence, the produced AgNPs can be directly used in various applications and indirectly reduced the hectic in downstream processing.

With the increasing awareness towards environmentally-friendly approach for synthesis of non-toxic AgNPs, problems such as producing polydispersible nanoparticles and slow production rate have plagued the biological synthesis approaches. Despite the stability and safety issues, monodispersity and nanoparticles sizes are the core for the synthesis of AgNPs. Hence, the present optimization study was conducted to investigate the effects of operating condition on AgNPs synthesis using a fungal strain, *Pycnoporus sanguineus* in batch mode.

Materials and Methods

Preparation and cultivation of *P. sanguineus*. Malaysian white-rot fungus *P. sanguineus* was obtained from the Forest Research Institute of Malaysia (FRIM), Selangor, Malaysia. The fungal strain was grown on malt extract agar plates at 30°C for 5 days and sub-cultured monthly. It was then maintained and preserved at 4°C. Fungi mycelial mat was suspended in 250 mL of sterile deionized water supplemented with 0.1% Tween-80 to yield a seed inoculum density of 10^8 spore mL^{-1}.

Biosynthesis of AgNPs. Fungus cultivation was prepared using nutrient medium comprised of (w/v): 1% yeast extract, 1% malt extract, and 2% glucose. Initial pH of the medium was adjusted to pH 5.6±0.2 using 1 M NaOH and 1 M HCl and then sterilized at 121°C for 15 min. Subsequently, 10% (v/v) seed inoculum was inoculated into each 50 mL medium in a 150 mL Erlenmeyer flasks. The flasks were incubated at 30°C, 200 rpm for 3 days. The cell-free filtrate was collected by centrifugation at 4500 rpm for 15 min and was then used as a source for AgNPs synthesis. Anionic surfactant sodium dodecyl sulphate (SDS) was added into 10^{-3} M silver nitrate ($AgNO_3$) to reduce agglomeration of AgNPs and to control the morphological evolution of AgNPs (Al-Thabaiti et al., 2008). Later, 100 mL of this mixture was treated with 1% (v/v) of cell-free filtrate in 250 mL Erlenmeyer flasks. The reaction mixtures were then incubated and tested according to the statistical design of the experiment. Nitrate reductase activity assay was carried out according to the method described by Redinbaugh and Campbell (1985) to determine the possible reduction mechanism route.

Characterization of AgNPs. The bioreduction of Ag^+ ion in samples were monitored by absorbance measurement using double beam UV-vis spectrophotometer (Shidmazu UV-2550, USA). According to Chan and Mashitah (2012), the absorbance band of AgNPs occurs between 430–450 nm. The average size of AgNPs in sample solutions were then measured using dynamic light scattering (DLS) a non-invasive back scatter (NIBS®) technology (Zetasizer Nano ZS, Malvern Instruments, UK). The morphologies of AgNPs synthesized were identified using transmission electron microscope (EFTEM, Zeiss Libra® 120 Plus, USA). The samples were dropped onto 300 mesh of carbon-coated copper grid and allowed to air dry prior to measuring using EFTEM.

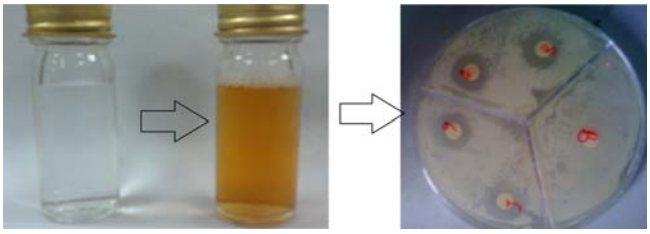

Fig. 1 Schematic diagram showing AgNPs formation after 3 days of incubation and disc diffusion assay.

The IR spectrum of synthesized AgNPs was obtained by using the Fourier Transform Infrared Spectrometer (IRPrestige-21, Shimadzu, Japan). Reflectance technique was used by mixing KBr and AgNPs at a ratio of 1:100 and compressing the mixture into a transparent disc. The disc was placed directly into the infrared spectrometer in the wave number range of 400–4000 cm^{-1}.

Antimicrobial Studies of AgNPs. AgNPs produced were tested for antimicrobial activity by disk diffusion assay against the pathogenic bacteria *Escherichia coli* (Gram-negative), *Staphylococcus aureus* and *Staphylococcus epidermidis* (Gram-positive), yeast *Candida albicans*, and fungi *A. niger*. The pure cultures of bacteria and fungi were sub-cultured on nutrient agar, and swabbed uniformly onto individual plates using sterile cotton swabs. Twenty milliliters of AgNPs were impregnated onto 6-mm sterile blank disc and allowed to dry before placing onto the culture plate. Bacterial-cultured plates were incubated at 37°C for 24 h, while the fungal-cultured plates were incubated at 30°C for 48 h. Fig 1 shows an example of disk diffusion assay of AgNPs produced after 3 days.

Statistical experimental design. One-factor-at-a-time method was employed to investigate the possible optimum levels of the influence operating condition that showed positive effects on AgNPs sizes. It is necessary because functionality of nanoparticles is inversely proportional to the size of the particles produced (Chan and Mashitah, 2011). The components investigated comprised of stabilizer-to-$AgNO_3$ concentration ratio, inoculum percentage, $AgNO_3$ concentration, temperature, and agitation. To obtain significant effect on the response (AgNPs size), stabilizer concentration was varied at 1, 2, 4, 5, 6, 8, and 10 mmol L^{-1} and $AgNO_3$ concentration at 1, 5, 10, 15, and 20 mmol L^{-1}. Cell-free inoculum, which is considered as an important factor for the bioreduction of AgNPs was varied at 1, 3, 5, 7, and 9 % (v/v). The

Table 1 Level of variables chosen for Box-Behnken design

Factor	Variable	Coded variable level		
		Low	Centre	High
		-1	0	+1
A	[$AgNO_3$], mmol L^{-1}	0.001	0.005	0.01
B	Temperature, °C	33	37	40
C	Agitation speed, rpm	150	200	250

reaction temperature was conducted at 32, 34, 36, 38, and 40°C, while the agitation was investigated at 50, 100, 150, 200, and 250 rpm.

Response Surface Methodology (RSM) is a collection of statistical and mathematical methods in solving and analyzing engineering related problems. This design procedure involves four important steps (Gunaraj and Murugan, 1999): namely designing and performing a series of experiment for adequate and reliable measurement of the response of interest, developing mathematical model of second order with the best fittings, finding the optimal set of experimental parameters that produce optimal value of response, and representing the direct and interactive effects of process parameters through graphical plots.

In the present study, the Box-Behnken experimental design under RSM developed by Design Expert software (Version 6.0.10, Stat-Ease, Inc., USA) was employed to optimize the three significant process variables namely $AgNO_3$ concentration, reaction temperature, and agitation speed. Other process variables were fixed from the result of the one-factor-at-a-time study. Box-Behnken design requires experiment number $N=k^2+k+c_p$, where k is the factor number and c_p is the replicate number of the central point (Souza Anderson et al., 2005). Hence, for a three-factor design, a total of 17 experimental runs were executed and their observations were fitted to the following second order polynomial model:

$$Y=\beta_0+\beta_1A+\beta_2B+\beta_3C+\beta_{11}A^2+\beta_{22}B^2+\beta_{33}C^3+\beta_{12}C^3+\beta_{12}AB+\beta_{13}AC+\beta_{12}BC$$

where Y is the dependent variable (size of AgNPs), A, B, and C are the independent variables, β_0 is the regression coefficient at center point, β_1, β_2, and β_3 are the linear coefficient; β_{11}, β_{22}, and β_{33} are the quadratic coefficients, and β_{12}, β_{13}, and β_{23} are the second order interaction coefficients. Table 1 shows the level of variable chosen for Box-Behnken design.

The developed model was evaluated using statistical analysis including analysis of variance (ANOVA), and Fisher's F-test. The quality of fit of the model equation was expressed by the coefficient of determination, R^2. The fitted model was then plotted in the form of contour and surface plots in order to illustrate the relationship between responses. A predicted optimum combination of the effects was generated using the statistical software package Design-Expert 6.0.10. Finally, sets of experiments were performed using the suggested optimum combination to validate the Box-Behnken model developed.

Results and Discussion

Bioreduction of silver occurred due to the presence of reducing agent, which reduced Ag^+ in $AgNO_3$ solution into Ag^0 of nanosize as in Equation 1 (Chan and Mashitah, 2012).

$$Ag^+ + e^- \rightarrow Ag_0 \quad (1)$$

In our study, when the reducing agent in cell-free filtrate of *P. sanguineus* was in-contact with $AgNO_3$ solution, it changed into yellowish brown color. It was reported that the enzyme reductase, nitrate reductase, hydrogenase or electron shuttle quinones were the potential enzymatic pathway for bioreduction of silver (Ottow and von Klopotek, 1969; Duran et al., 2005). Positive results were obtained during nitrate reductase assay. Hence, it can be deduced that nitrate reductase serves as a reducing agent for the reaction in equation (1). The formation of silver can be identified through visible observation in the change of color of the solution during the reaction from colorless to pale yellow or dark brown (Sathishkumar et al., 2009). The change in color indicates the presence of AgNPs in solution due to the excitation of surface plasmon vibration (Rai et al., 2006). Further confirmation can be conducted using UV-vis spectral analysis, where surface absorption band of AgNPs was determined at 420 nm.

Determination of the optimum levels parameters using one-factor-at-a-time (OFAT) method. OFAT was used to determine the possible optimum level of parameters for AgNPs production, among which stabilizer concentration, inoculum percentage, $AgNO_3$ concentration, temperature, and agitation were chosen to obtain the optimum level. Anion sodium dedocyl sulfate (SDS) was used as a stabilizer. Anion SDS having a negative charge has the tendency to attach on to the synthesized AgNPs by forming micelles. It can also avoid AgNPs from precipitation as micelles would form suspension in liquid (Cui et al., 2008). Fig. 2 shows the effect of SDS concentration on AgNP size; the size of AgNP increased with increasing SDS concentration. At lower dosage, the AgNPs capped with SDS and tended to agglomerate over time, whereas at higher dosage, the hydrodynamic sizes of AgNPs recorded were exceptionally higher than the AgNPs core itself. However, the results herein deviated from those obtained by López-Miranda et al. (2012), who showed that low concentration of SDS promotes highly polydisperse nanoparticles with large mean size. This may be due to the presence of SO_3^{2-}, which serves as a reducing agent. The AgNPs capped with 5 mmol L^{-1} of SDS was found to have the most stable hydrodynamic sizes of AgNPs over the tested time. Hence, SDS concentration of 5 mmol L^{-1} was chosen for further optimization studies.

In most cases, during the synthesis of AgNPs, the effect of reducing agent concentration was less studied. Nanda and Saravanan (2009) have challenged 1% (v/v) supernatant of the bacteria culture *S. aureus* with $AgNO_3$, whereas other researchers investigated on the biosynthesis of AgNPs using 5% (w/v) biomass fungus *Aspergillus flavus* for the synthesis (Vigneshwaran et al., 2007). Because the enzymatic reduction is one of the

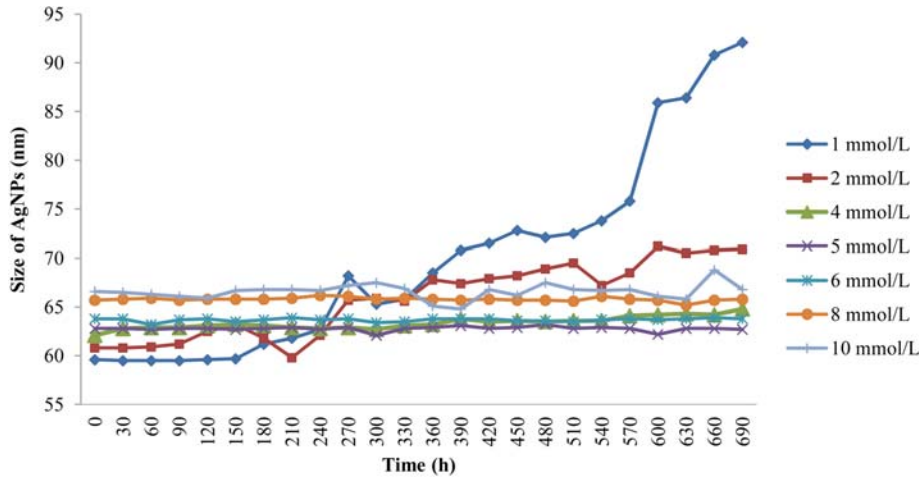

Fig. 2 Effects of sodium dedocyl sulfate (SDS) concentration on the size of AgNPs.

possible routes for biosynthesis of AgNPs, studies on the effects of a reducing agent become crucial. The mechanism widely acknowledged is the presence of nitrate reductase enzyme, which serves as a reducing agent (Anil Kumar et al., 2007; Kalimuthu et al., 2008). Nitrate reductase is a molybdoenzyme that reduces nitrate (NO_3^-) to nitrite (NO_2^-) in the nitrogen cycle (Tavares et al., 2006). Furthermore, Morozkina et al. (2005) reported that fungi were capable of producing the enzyme nitrate reductase. Thus, it is important to find the appropriate concentration of reducing agent that can affect the production of AgNPs. In the present study, different percentages of inoculum, which served as reducing agent supplier, were prepared, and their capabilities in producing different sizes of AgNPs were evaluated. Fig. 3A shows that nanoparticles size decreased from 63.79±5.38 to 24.55±5.75 nm when the inoculum size increased from 1 to 5%. Beyond this level, not much difference was observed. Hence, 5% inoculum size was the breaking point to give smallest particle size at 63.3 nm.

Besides the reducing agent, substrate concentration is also another notable feature in determining the AgNPs size. Korbekandi et al. (2012) reported that increased in $AgNO_3$ concentration would result in smaller nanoparticle size production. However, Fig. 3B shows that as increased in $AgNO_3$ concentration does not produced smaller AgNPs, most likely due to the increase in toxic metal ion (Ag^+) concentration. Although Nabeel et al. (2005) reported that fungal biomass has the capability in detoxification of Ag^+, detoxification mechanism using fungi culture is still unknown. As shown in Equation (1), nitrate reductase facilitated the reduction of Ag^+ by releasing an electron for the formation of AgNPs. Based on the above stoichiometic, nitrate reductase has to be present in excess in order to facilitate the bioreduction reaction. Increase in $AgNO_3$ concentration caused nitrate reductase to become a limiting factor, hence producing larger AgNPs with higher Ag^+ concentration. Fig. 3B also shows that 5% culture supernatant is able to detoxify 1 mmol L^{-1} of $AgNO_3$.

Most researches conducted on the effects of temperature on AgNPs corresponded to the UV-vis spectral. Kaviya et al. (2011) reported that as the reaction temperature increased, surface plasmon resonance band shifted to the lower wavelength, which indicated the reduction of mean diameter of biogenic AgNPs. This phenomenon was also reported during biosynthesis of AuNPs; increased in reaction temperature leads to increase in the reaction rate and decreased in particle size (Rai et al., 2006; Song et al., 2009). In the present study, the effects of temperature on AgNPs size were studied, and the results were in agreement with those conducted by other researchers (Mohammed Fayaz et al., 2009; Puchalski et al., 2009; de Assumpção et al., 2010). Fig. 3C shows that as the temperature increased from 32 to 40°C, the particles size decreased from 44.64±4.21 nm to 16.78±2.82 nm. It was also observed visually that as the reaction temperature increased, the rate of reaction also increased with respect to the color intensity formed.

Another important parameter which influenced the production of AgNPs was the agitation speed. When dealing with microbial cultivation, agitation speed controls the aeration rate and dissolved oxygen concentration (Yan et al., 2005). In AgNPs synthesis, aeration was not an important factor for controlling agitation speed, but maximized the reaction surface and provided a homogenous suspension environment (Armenante and Nagamine, 1998). Fig. 3D shows that the size of AgNPs decreased to 14.54±1.01 nm with increased agitation speed at 250 rpm. Higher agitation speed provided a more homogenous suspension environment and hence increased the reaction surface area. Because the aim of using OFAT was to select the important factors and minimize the number of factors for optimization studies using Box-Behnken, only three factors, namely $AgNO_3$ concentration, incubation temperature, and agitation speed were identified as the most influencing factors while keeping other parameters constant at the optimum value found in one-factor-at-one-time (OFAT).

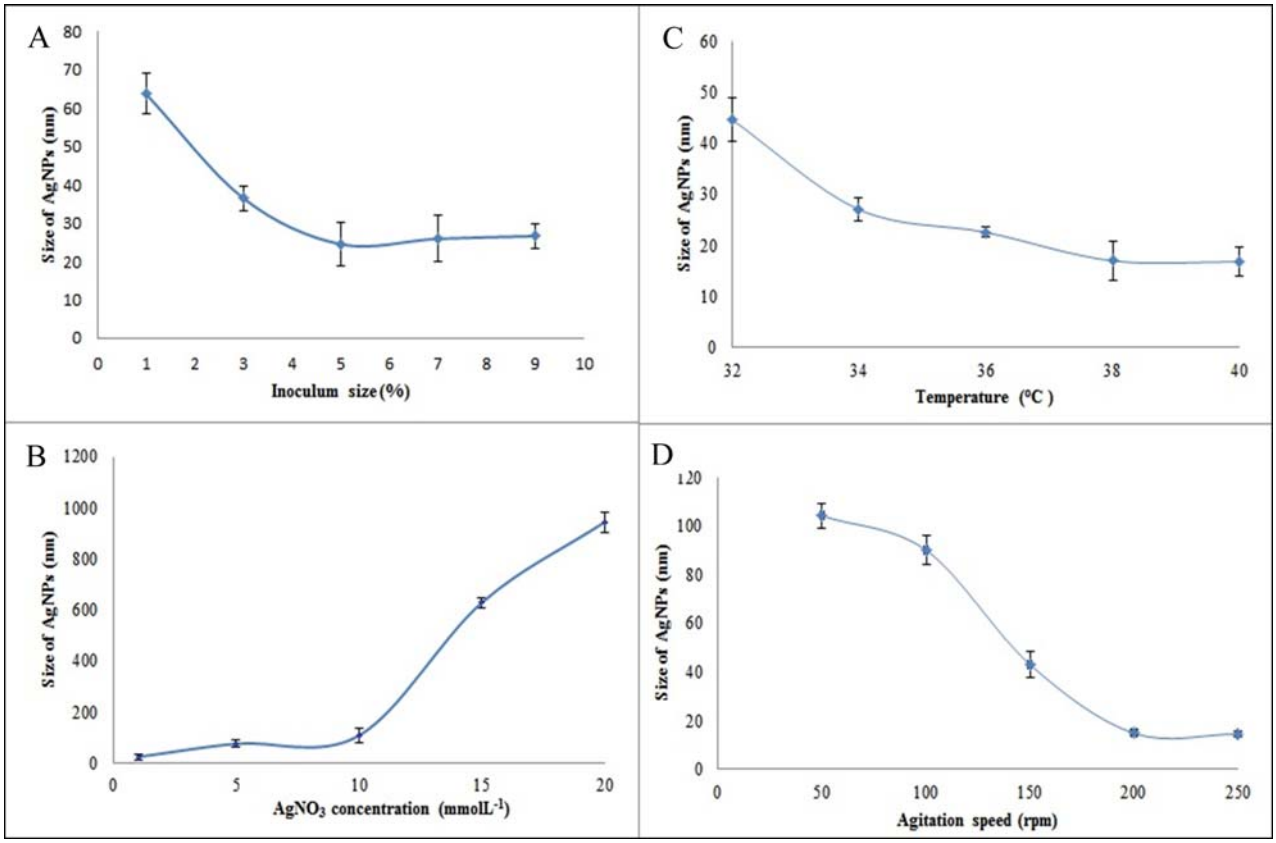

Fig. 3 (A) Effects of inoculum size on the size of AgNPs, (B) Effects of $AgNO_3$ concentration on the size of AgNPs, (C) Effects of temperature on the size of AgNPs, (D) Effects of agitation speed of the size of AgNPs.

Table 2 Experimental design using Box-Behnken showing coded and actual values along with the experimental and predicted responses

Run order	$[AgNO_3]$ mmol L^{-1}	Temperature (°C)	Agitation speed rpm	AgNPs size (nm)	
				Experimental	Predicted
1	1	33	200	32.40	36.00
2	10	33	200	49.80	53.22
3	1	40	200	20.48	17.06
4	10	40	200	72.80	69.20
5	1	36.5	150	62.90	61.88
6	10	36.5	150	96.68	95.84
7	1	36.5	250	16.85	17.70
8	10	36.5	250	52.09	53.11
9	5.5	33	150	70.58	68.00
10	5.5	40	150	70.59	75.03
11	5.5	33	250	37.50	33.06
12	5.5	40	250	20.48	23.06
13	5.5	36.5	200	25.90	32.61
14	5.5	36.5	200	38.72	32.61
15	5.5	36.5	200	32.80	32.61
16	5.5	36.5	200	35.80	32.61
17	5.5	36.5	200	29.85	32.61

Optimization of process parameters by response surface methodology (RSM). Based on the OFAT experiment, Box-Behnken design under response surface methodology was used to determine the optimum condition of the three significant factors in

Table 3 Analysis of variance of quadratic model for AgNPs synthesis

Source	Sum of squares	*F*-value	Prob>F
Model	8017.170	30.30	<0.0001
A	2405.98	81.84	<0.0001
B	4.39	0.15	0.7106
C	3777.11	128.48	<0.0001
A^2	364.17	12.39	0.0097
B^2	16.11	0.55	0.4832
C^2	974.95	33.16	0.0007
AB	304.85	10.37	0.0146
AC	0.53	0.018	0.8969
BC	72.48	2.47	0.1404
Lack of fit	105.6	1.41	0.3640

R^2=0.9750 , adjusted R^2=0.9428, adequate precision=18.945

order to produce smallest sized AgNPs. For each run, the experiment along with the predicted particle size obtained from the regression equation for the 17 combinations are shown in Table 2. For predicting the optimal values of AgNPs synthesis within the experimental constrains, a second order polynomial model was fitted to the experimental results by Design Expert software. The model developed was expressed as follows:

$$Y\ (\text{AgNPs size, nm}) = 32.61 + 17.34A - 0.74B - 21.73C + 9.30A^2 + 1.96B^2 + 15.22C^2 + 8.73AB + 0.36AC - 4.26BC \quad (2)$$

where the AgNPs size as yield (Y) was a function of $AgNO_3$ concentration (A), incubation temperature (B), and agitation speed (C).

The significance and adequacy of the model were checked

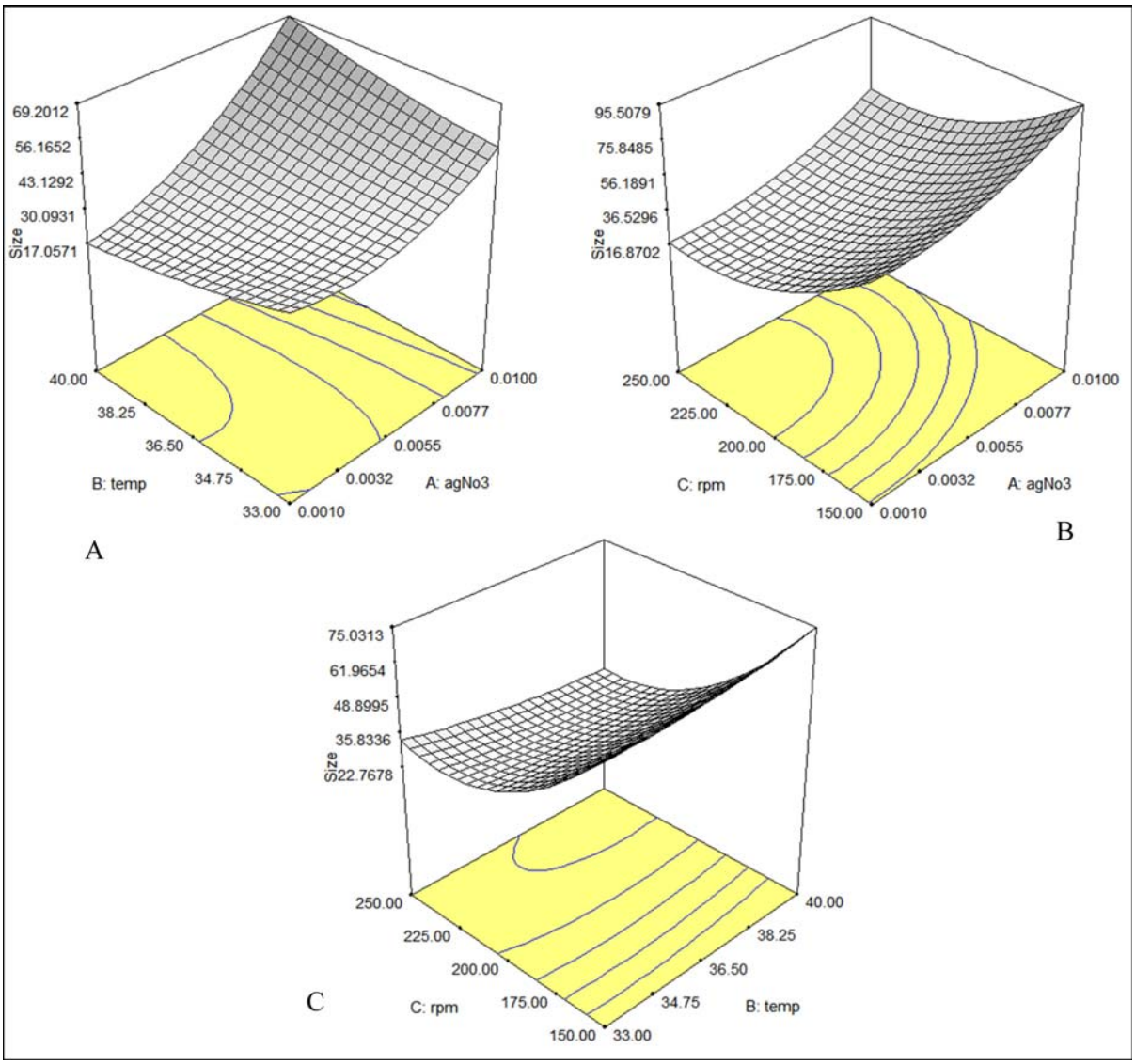

Fig. 4 The 3D response surface curves of the combined effects of [$AgNO_3$], temperature, and agitation speed on AgNPs synthesis: (A) [$AgNO_3$] and temperature at fixed level of agitation speed (200 rpm), (B) [$AgNO_3$] and agitation speed at fixed level of temperature (33℃), and (C) temperature and agitation speed at fixed level of [$AgNO_3$] at 1 mM.

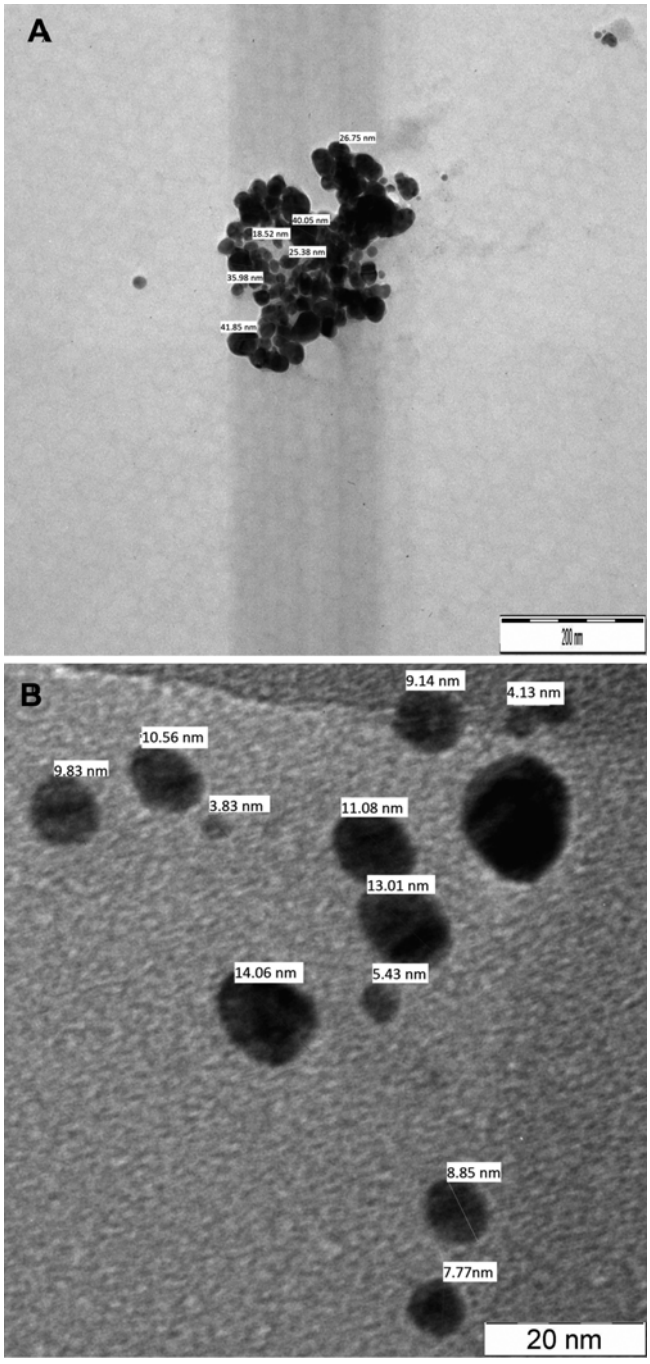

Fig. 5 TEM micrograph: (A) AgNPs before optimization and (B) AgNPs after optimization

through the analysis of variance (ANOVA) using Fisher's statistical analysis (Table 3). The model *F*-value of 30.30 and *p*-value of <0.0001 for AgNPs synthesis imply that the model is statistically significant. There was only a 0.01% chance that a model *F*-value could occur due to noise. The value with Prob >*F* less than 0.05 indicated that the model terms are also significant, whereas those greater than 0.10 are insignificant. In this case, A, C, A^2, C^2, and AB are significant model terms. The high coefficient of determination (R^2) and adjusted R^2 of 0.9750 and 0.9428 indicated the efficacy of the model, suggesting that 97.50 and 94.28% variation could be accounted by the model equation. Hence, a good statistical model should result in R^2~1 (Reddy et al., 2008). Adequate precision measures the signal to noise ratio, and a value >4 is desirable. The ratio of 18.945 indicated an adequate signal; therefore, the model was significant for the process.

The 3D response surface plot was the graphical representations of the regression equation used to investigate the interaction among three variables and to determine the optimum parameter to synthesis smallest sized AgNPs. Significance of the interaction plots between the corresponding variables was indicated by an elliptical or saddle nature of the contour plots (Muralidhar et al., 2001). Fig. 4A represents the interaction between [$AgNO_3$] and temperature. Note that the minimum AgNPs size was obtained at lower $AgNO_3$ concentration and higher incubation temperature. Fig. 4B shows the 3D plot corresponding to [$AgNO_3$] and agitation speed, and this plot did not show clearly how both factors interacted; hence there was no significant interaction between both factors. Similarly Fig. 4C also did not show clearly any interaction between temperature and agitation. However this phenomenon can also mean that the optimized combinations of the selected process parameters showed strong synergistic effects on producing the smallest size of AgNPs.

The smallest size of AgNPs at 7.02 nm was predicted by solving the model at the optimum condition of $AgNO_3$ concentration 1 mmol L^{-1}, temperature 40°C, and agitation speed of 230 rpm. In order to verify the optimization results and to validate the model developed, a set of experiment with five replicates was conducted according to the parameters stated in Table 4. From the validation, the smallest AgNPs obtained was 7.58 nm, which was slightly higher than the predicted value. The slight deviation may be explained based on the experimental conditions, in which the experiments were run in the three equal technological space considered in Box-Behnken.

Characterizations. TEM micrographs were taken to investigate the difference between un-optimized and optimized size of AgNPs. Fig. 5A shows that AgNPs produced before optimization tend to agglomerate with average nanoparticle size of 26.82 nm, whereas Fig. 5B shows that AgNPs synthesized using optimum parameter were more monodispersed with average particle size of 7.46 nm. Fig. 6 and Table 6 show the FTIR spectra and the major peaks wavelength for both AgNPs functionalized with SDS and control AgNPs. The two troughs observed in the regions 2935.66 and 1238.30 cm^{-1} result from the aliphatic C-H group and asymmetric bending of SO_3 (Saad et al., 2012) of SDS and is not observed from the control AgNPs. Hence, the results suggested that anionic SO_3 serving as an important functional group is involved in stabilization.

Silver has an important antimicrobial effect and has been used since the Roman times. These antimicrobial effects are reported to be dependent of superficial contact, hence inhibiting the enzymatic

Table 4 Validation of experimental model

Experiment	[$AgNO_3$] nnol L^{-1}	Temperature (°C)	Agitation speed rpm	AgNPs size (nm)		% error
				Experimental	Predicted	
1	1	40	230	7.58	7.02	7.26
2	1	38.7	232	10.52	9.84	6.91
3	1	38.7	246	10.28	9.44	8.90
4	1	38.1	231	12.81	11.72	9.30
5	1	37.6	233	14.21	13.04	9.87

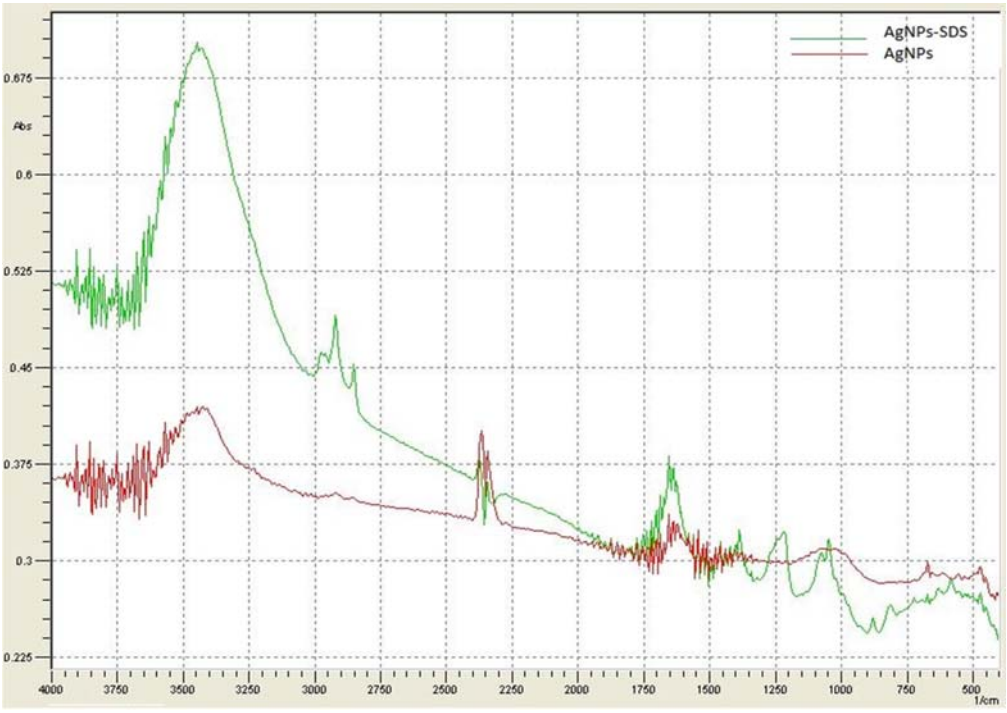

Fig. 6 Fourier transform spectroscopy spectra of control AgNPs and AgNPs-SDS.

Table 5 Disc diffusion assay between un-optimized and optimized AgNPs synthesis conditions

Tested microorganism	Inhibition zone (cm)	
	Un-optimized condition	Optimized condition
E. coli	1.30±0.02	3.82±0.05
S. aureus	1.15±0.01	1.73±0.01
S. epidermis	0.80±0.00	1.80±0.03
C. albicans	0.95±0.01	3.31±0.02
A. niger	No inhibition	3.00±0.02

Table 6 Fourier transforms infrared spectroscopy spectra characteristic and functional groups

Major peak	Wavelength (cm^{-1})		Assignment
	Control AgNPs	AgNPs-SDS	
1	-	1238.30	Asymmetric bending of SO_3
2	1624.06	1634.35	C=O stretching
3	-	2935.66	Aliphatic C-H group
4	3433.29	3444.87	Hydroxyl

respiratory system of microbes and altering DNA synthesis (Hidalgo and Dominguez, 1998; Brett, 2006). In the present study, the antimicrobial effects of AgNPs produced under both optimized and un-optimized conditions were conducted. Results showed that AgNPs synthesized by *sanguineus* using optimized conditions were stronger antimicrobial and antifungal agents compared to AgNPs synthesized under un-optimized condition.

Three parameters; $AgNO_3$ concentration, incubation temperature, and agitation speed were selected for AgNPs synthesis using *P. sanguineus*. These parameters were first optimized by the OFAT method and later by Box-Behnken under RSM. Results obtained critically point out the importance of $AgNO_3$ concentration (1 mmol L^{-1}), temperature (40°C), and agitation speed (230 rpm) for the production of AgNPs by *P. sanguineus* of particle sized 7.58 nm, which is 8.6-fold smaller than the un-optimized AgNPs. The antimicrobial assay also concluded that AgNPs produced using optimum conditions have better biocide power. The experimental

data were found to fit well with the model predicted values with less than 10% error.

Acknowledgment. The authors are grateful to the School of Chemical engineering for providing the lab facilities, USM-PRGS Grant, USM Fellowship and Research University Grant 1001/PJKIMIA/814162 for financing this research project.

References

Ahmad A, Mukherjee P, Senapati S, Mandal D, Khan MI, Kumar R et al. (2003a) Extracellular biosynthesis of silver nanoparticles using the fungus *Fusarium oxysporum*. *Colloids Surf B* **28**, 313–8.

Ahmad A, Senapati S, Khan MI, Kumar R, and Sastry M (2003b) Extracellular biosnythesis of monodisperse gold nanoparticles by a novel extremophilic actinomycete, *Thermomonaspora sp. Langmuir* **19**, 3550–3.

Al-Thabaiti SA, Al-Nowaiser FM, Obaid AY, Al-Youbi AO, and Khan Z (2008) Formation and characterization of surfactant stabilized silver nanoparticles: A kinetic study. *Colloids Surf B* **67**, 230–7.

Anil Kumar S, Abyaneh MK, Gosavi SW, Kulkarni SK, Pasricha R, Ahmad A et al. (2007) Nitrate reductase-mediated synthesis of silver nanoparticles from AgNO3. *Biotechnol Lett* **29**, 439–45.

Armenante PM and Nagamine EU (1998) Effect of low off-bottom impeller clearance on the minimum agitation speed for complete suspension of solids in stirred tanks. *Chemical Eng Sci* **53**, 1757–75.

Balaji D, Basavaraja S, Deshpande R, Mahesh D, Prabhakar B, and Venkataraman A (2009) Extracellular biosynthesis of functionalized silver nanoparticles by strains of Cladosporium cladosporioides fungus. *Colloids Surf B* **68**, 88–92.

Beveridge TJ, Hughes MN, Lee H, Leung KT, Poole RK, Savvaidis I et al. (1996) Metal-Microbe Interactions: Contemporary Approaches. In *Advances in Microbial Physiology*. Poole RK (ed.), vol. 38, pp. 177–243. Academic Press, New York, USA.

Bhainsa KC and D'Souza SF (2006a) Extracellular biosynthesis of silver nanoparticles using the fungus *Aspergillus fumigatus*. *Colloids Surf B* **47**, 160–4.

Bhainsa KC and D'Souza SF (2006b) Extracellular biosynthesis of silver nanoparticles using the fungus Aspergillus fumigatus. *Colloids Surf B* **47**, 160–4.

Brett DW (2006) A discussion of silver as an antimicrobial agent: alleviating the confusion. *Ostomy Wound Manag* **52**, 34–41.

Bruins MR, Kapil S, and Oehme FW (2000) Microbial Resistance to Metals in the Environment. *Ecotoxicol Environ Saf* **45**, 198–207.

Chan YS and Mashitah MD (2011) A Macro View of Bionanotechnology: Application and Implicatins in the Near Future. *J Bionanoscience* **5**, 97–106.

Chan YS and Mashitah MD (2012) Instantaneous Biosynthesis of Silver Nanoparticles by Selected Macro Fungi. *J Basic Appl Sci* **6**, 222–6.

Chang JY, Chang JJ, Lo B, Tzing SH, and Ling YC (2003) Silver nanoparticles spontaneous organize into nanowires and nanobanners in supercritical water. *Chem Phys Lett* **379**, 261–7.

Cui ZG, Shi KZ, Cui YZ, and Binks BP (2008) Double phase inversion of emulsions stabilized by a mixture of CaCO3 nanoparticles and sodium dodecyl sulphate. *Colloids Surf A* **329**, 67–74.

de Assumpção TAA, da Silva DM, Kassab LRP, Martinelli JR, and de Araújo CB (2010) Influence of the temperature on the nucleation of silver nanoparticles in Tm^{3+}/Yb^{3+} codoped $PbO\text{-}GeO_2$ glasses. *J Non-Cryst Solids* **356**, 2465–7.

Duran N, Marcato PD, Alves OL, Souza GI, and Esposito E (2005) Mechanistic aspects of biosynthesis of silver nanoparticles by several Fusarium oxysporum strains. *J Nanobiotechnology* **3**, 8.

Gade AK, Bonde P, Ingle AP, Marcato PD, Durán N, and Rai MK (2008) Exploitation of *Aspergillus niger* for synthesis of silver nanopartices. *J Biobased Mater Bio* **2**, 243–7.

Greulich C, Diendorf J, Simon T, Eggeler G, Epple M, and Köller M (2011) Uptake and intracellular distribution of silver nanoparticles in human mesenchymal stem cells. *Acta Biomater* **7**, 347–54.

Gunaraj V and Murugan N (1999) Application of response surface methodology for predicting weld base quality in submerged arc welding of pipes. *J Mater Process Tech* **88**, 266–75.

Gurunathan S, Kalishwaralal K, Vaidyanathan R, Venkataraman D, Pandian SRK, Muniyandi J et al. (2009) Biosynthesis, purification and characterization of silver nanoparticles using Escherichia coli. *Colloids Surf B* **74**, 328–35.

Hidalgo E and Dominguez C (1998) Study of cytotoxicity mechanisms of silver nitrate in human demal fibroblasts. *Toxicol Lett* **15**, 169–79.

Jia H, Zeng J, Song W, An J, and Zhao B (2006) Preparation of silver nanoparticles by photo-reduction for surface-enhanced Raman scattering. *Thin Solid Films* **496**, 281–7.

Kalimuthu K, Babu RS, Venkataraman D, Bilal M, and Gurunathan S (2008) Biosynthesis of silver nanocrytals by *Bacillus licheniformis*. *Colloids Surf B* **65**, 150–3.

Kalishwaralal K, Deepak V, Ramkumarpandian S, Nellaiah H, and Sangiliyandi G (2008) Extracellular biosynthesis of silver nanoparticles by the culture supernatant of *Bacillus licheniformis*. *Materials Lett* **62**, 4411–3.

Kannan N, Mukunthan KS, and Balaji S (2011) A comparative study of morphology, reactivity and stability of synthesized silver nanoparticles using Bacillus subtilis and Catharanthus roseus (L.) G. Don. *Colloids Surf B* **86**, 378–83.

Kaviya S, Santhanalakshmi J, and Viswanathan B (2011) Green synthesis of silver nanoparticles using *Polyalthia longifolia* leaf extract along with D-sorbitol study of antibacterial activity. *J Nanotechnology* **2012**, ID 152970.

Khanna PK, Singh N, Charan S, Subbarao VVVS, Gokhale R, and Mulik UP (2005) Synthesis and characterization of Ag/PVA nanocomposite by chemical reduction method. *Mater Chem Phys* **93**, 117–21.

Klaus-Joerger T, Joerger R, Olsson E, and Granqvist C-G (2001) Bacteria as workers in the living factory: metal-accumulating bacteria and their potential for materials science. *Trends Biotechnol* **19**, 15–20.

Korbekandi H, Iravan S, and Abbasi S (2012) Optimization of biological synthesis of silver nanoparticles using *Lactobacillus casei* subsp. *casei*. *J Chem Technol Biot* **87**, 932–7.

Long D, Wu G, and Chen S (2007) Preparation of oligochitosan stabilized silver nanoparticles by gamma irradiation. *Radiat Phys Chem* **76**, 1126–31.

López-Miranda A, López-Valdivieso A, and Viramontes-Gamboa G (2012) Silver nanoparticles synthesis in aqueous solutions using sulfite as reducing agent and sodium dodecyl sulfate as stabilizer. *J Nanopart Res* **14**, 1–11.

Meyer JN, Lord CA, Yang XY, Turner EA, Badireddy AR, Marinakos SM et al. (2010) Intracellular uptake and associated toxicity of silver nanoparticles in *Caenorhabditis elegans*. *Aquat Toxicol* **100**, 140–50.

Mohammed Fayaz A, Balaji K, Kalaichelvan PT, and Venkatesan R (2009) Fungal based synthesis of silver nanoparticles—An effect of temperature on the size of particles. *Colloids Surf B* **74**, 123–6.

Mokhtari N, Daneshpajouh S, Seyedbagheri S, Atashdehghan R, Abdi K, Sarkar S et al. (2009) Biological synthesis of very small silver nanoparticles by culture supernatant of Klebsiella pneumonia: The effects of visible-light irradiation and the liquid mixing process. *Mater Res Bull* **44**, 1415–21.

Morozkina E, Kurakov A, Nosikov A, Sapova E, and L'vov N (2005) Properties of nitrate reductase from *Fusarium oxysporum* 11dn1 fungi grown under aerobic and anaerobic condition. *Prikl Biokhim Mikrobiol* **41**, 292–7.

Muralidhar RV, Chirumamila RR, Marchant R, and Nigam P (2001) A response surface approach for the comparison of lipase production by

Candida cylindracea using two different carbon sources. *Biochem Eng J* **9**, 17–23.

Nabeel MA, Sastry KS, and Mohan PM (2005) Biosorption of silver ions by processed *Aspergillus niger* biomass. *Biotechnol Lett* **17**, 551–6.

Nanda A and Saravanan M (2009) Biosynthesis of silver nanoparticles from Staphylococcus aureus and its antimicrobial activity against MRSA and MRSE. *Nanomed-Nanotechnol* **5**, 452–6.

Ottow JCG and von Klopotek A (1969) Enzymatic reduction of iron oxide by fungi. *Appl Microbiol* **18**, 41– 3.

Puchalski M, Kowalczyk PJ, Zasada I, Krukowski P, and Olejniczak W (2009) Alloying process at the interface of silver nanoparticles deposited on Au (1 1 1) substrate due to the high-temperature treatments. *J Alloy Compd* **481**, 486–91.

Rai A, Singh AK, Ahmad A, and Sastry M (2006) Role of halide ions and temperature on the morphology of biologically synthesized gold nanotriangles. *Langmuir* **22**, 736–41.

Rajesh Kumar R, Poornima Priyadharsani K, and Thamaraiselvi K (2012) Mycogenic synthesis of silver nanoparticles by the Japanese environmental isolate Aspergillus tamarii. *J Nanopart Res* **14**, 1–7.

Rao JP and Geckeler KE (2011) Polymer nanoparticles: Preparation techniques and size-control parameters. *Prog Polyme Sci* **36**, 887–913.

Reddy LVA, Wee Y-J, Yun J-S, and Ryu H-W (2008) Optimization of alkaline protease production by batch culture of Bacillus sp. RKY3 through Plackett-Burman and response surface methodological approaches. *Bioresource Technol* **99**, 2242–9.

Redinbaugh MG and Campbell WH (1985) Quaternary Structure and Composition of Squash NADH: Nitrate Reductase. *J Biol Chem* **260**, 3380–5.

Saad P, Flach CR, Walters RM, and Mendelsohn R (2012) Infrared spectroscopic studies of sodium dodecyl sulfate permeation and interaction with stratum corneum lipid in skin. *Int J Cosmetic Sci* **34**, 36–43.

Sathishkumar M, Sneha K, Won SW, Cho CW, Kim S, and Yun YS (2009) Cinnamon zeylanicum bark extract and powder mediated green synthesis of nano-crystalline silver particles and its bactericidal activity. *Colloids Surf B* **73**, 332–8.

Song JY, Jang H-K, and Kim BS (2009) Biological synthesis of gold nanoparticles using *Magnolia kobus* and *Diopyros kaki* leaf extracts. *Process Biochem* **44**, 1133–8.

Souza Anderson S, dos Santos Walter N, and Ferreira Sergio L (2005) Application of Box-Behnken design in the optimization of an on-line pre-concentration system using knotted reactor for cadmium determination by flame atomic absorption spectrometry. *Spectrochim Acta B* **607**, 737–42.

Tavares P, Pereira AS, Moura JJG, and Moura I (2006) Metalloenzymes of the denitrification pathway. *J Inorg Biochem* **100**, 2087–100.

Vigneshwaran N, Ashtaputre NM, Varadarajan PV, Nachane RP, Paralikar KM, and Balasubramanya RH (2007) Biological synthesis of silver nanoparticles using the fungus Aspergillus flavus. *Mater Lett* **61**, 1413–8.

Vigneshwaran N, Kathe AA, Varadarajan PV, Nachane RP, and Balasubramanya RH (2006) Biomimetics of silver nanoparticles by white rot fungus, *Phaenerochaete chrysosporium. Colloids Surf B* **53**, 55–9.

Yan G, Du G, Li Y, Chen J, and Zhong J (2005) Enhancement of microbial transglutaminase production by Streptoverticillium mobaraense: application of a two-stage agitation speed control strategy. *Process Biochem* **40**, 963–8.

Yu C, Zhou X, and Gu H (2010) Immobilization, direct electrochemistry and electrocatalysis of hemoglobin on colloidal silver nanoparticles-chitosan film. *Electrochim Acta* **55**, 8738–43.